JOURNAL OF PROPULSION AND POWER
Vol. 20, No. 6, November–December 2004

Oxidation Processes and Phase Changes in Metastable Al–Mg Alloys

M. Schoenitz* and E. Dreizin†
New Jersey Institute of Technology, University Heights, Newark, New Jersey 07102

Oxidation behavior of metastable mechanical alloys in the Al–Mg binary system has been examined in the context of high-energy density materials and combustion applications. Mechanical alloy powders with compositions ranging from $Al_{0.95}Mg_{0.05}$ to $Al_{0.5}Mg_{0.5}$, as well as the component metals, were heated at 20 K/min in oxygen. Differential thermal analysis and thermogravimetric analysis showed that oxidation proceeds in two separate steps. During the first step occurring over the range of 550–600°C, Mg is oxidized and thereby quantitatively removed from the metallic phase. The selective removal of Mg from the alloy was identified by correlation of weight gain with the Mg concentration of the alloy and by x-ray diffraction and scanning electron microscopy, of intermediate products. The second step, during which the remainder of the metallic phase is oxidized, occurs over a wider range of temperatures (900–1200°C). The temperatures of both effects decrease slightly with increasing Mg content in the alloy. Oxidation is increasingly incomplete as the Mg concentration of the alloy decreases below 30 at.%. It was concluded that the low-temperature selective oxidation of Mg is controlled by the volatilization of Mg from the alloy. No correlation could be established between the oxidation reactions and subsolidus phase transitions, which occur over the temperature range of 100–400°C and are associated with the relaxation of the metastable state of the mechanical alloys.

Introduction

METALLIC additives to energetic formulations in propellants, explosives, or pyrotechnics are known to improve performance due to their high combustion enthalpies.[1–3] However, the full potential of metallic fuels is not easily exploited, mainly due to slow kinetics that lead to long ignition delays, high ignition temperatures, and incomplete combustion. Metastable metal-based materials have been proposed to improve overall ignition and combustion rates due to additional metastable phase transitions occurring before or during combustion.[4] Recently some of these materials, for example metal–metal and metal–gas supersaturated solid solutions, have been prepared using mechanical alloying, and their combustion behavior was compared to that of pure metals in both laminar aerosol flame and constant volume explosion experiments.[5–7] The results confirmed the hypothesis that the combustion rates can be significantly accelerated, and further research and development aimed at the optimization of the composition and phase makeup of the new metal-based materials, as well as their scaled-up and economically feasible manufacturing, seem to be warranted. At the same time, the mechanisms of ignition and combustion of the new materials need to be well understood and the correlations between the phase changes occurring in the new materials and observed ignition and combustion events need to be described.

One of the first metastable intermetallic systems investigated for combustion applications was the binary system Al–Mg. Earlier combustion experiments using commercial Al–Mg alloys have been reported in the literature[8]; however, no coherent picture regarding their combustion mechanism has emerged. Higher rates of flame propagation have been observed recently for aerosols of metastable supersaturated solid solutions (mechanical alloys) of Mg in Al, compared to the rates of flame propagation for aluminum and even magnesium aerosols with the same particle size.[6] Rates of pressure rise in constant volume explosion experiments were higher for mechanical alloys than for powder mixtures with identical bulk composition, or for powders of thermodynamically stable alloys.[7] The ignition temperatures of Al–Mg mechanical alloys were found to be much lower than that of pure Al, even at Mg concentrations as low as 5 at. %[5]. The phase changes occurring during heating of the mechanically alloyed supersaturated solid Al–Mg solutions were investigated in a separate study.[9] It was found that these mechanical alloys undergo a number of subsolidus-phase transitions associated with the formation of equilibrium intermetallic phases (at temperatures below the eutectic melting point of 450°C) when heated slowly in an inert atmosphere. Most of these phase transitions are exothermic and could play a role in accelerating ignition of the mechanical alloy particles.

One of the objectives of this research is to determine whether oxidation substantially affects the identified subsolidus phase changes so that ignition models considering the effect of the phase changes could be developed in the future. This research also aims to provide qualitative and quantitative information on the initial oxidation of Al–Mg mechanical alloys, which is needed for further development of ignition models for powders of these materials. The approach of this investigation is to use controlled sample heating in oxidative environment and exploit differential scanning calorimetry (DSC) or differential thermal analysis (DTA) combined with thermogravimetric analysis (TGA) to monitor phase changes and oxidation reactions. At the same time, intermediate reaction products are collected and analyzed using scanning electron microscopy (SEM) and x-ray diffraction (XRD).

Experimental

Three types of materials were investigated and compared to one another: a set of metastable Al–Mg mechanical alloys, a set of thermodynamically stable Al–Mg intermetallics with the same bulk compositions as the metastable alloys, and, finally, the pure metals Al and Mg.

Sample Preparation

Pure Al (Alfa Aesar, 98%, 10–14 μm) and Mg (Alfa Aesar, 99%, −325 mesh) powders were used as starting materials for the production of mechanical alloys and for thermal analysis of the component metals. Mechanical alloys with the compositions $Al_{0.95}Mg_{0.05}$, $Al_{0.9}Mg_{0.1}$, $Al_{0.8}Mg_{0.2}$, $Al_{0.7}Mg_{0.3}$, $Al_{0.6}Mg_{0.4}$, and $Al_{0.5}Mg_{0.5}$ were prepared in a SPEX 8000 high-energy ball mill. A zirconia vial and

Received 1 January 2003; accepted for publication 11 December 2003.

*Assistant Research Professor, Department of Mechanical Engineering. Member AIAA.
†Associate Professor, Department of Mechanical Engineering. Member AIAA.

zirconia balls were used to provide a chemically clean environment during milling. Batches of 10 g of each material were milled under Ar atmosphere, limited by the size of the milling vials and by safety considerations. Balls were 10 mm in diameter, with a ball-to-powder mass ratio of 5. Size and total weight of the balls affect the milling time required to achieve the final state[9]; a milling time of 12 h was required in the present study. Furthermore, 2 wt % of stearic acid [CH_3-$(CH2)_{16}$–COOH] was added during milling as a process control agent (PCA) to act against the formation of large agglomerates and to balance fracturing and cold welding in the sample powders. Milling usually raises the temperature of the sample to 50–60°C. After milling, the vials were cooled in room air and slowly vented. The powders were then dried at room temperature under a 25-in. Hg vacuum to remove excess PCA. The obtained mechanical alloys show some contamination (<1 wt %) of ZrO_2, introduced by the milling media. Oxygen levels in the as-synthesized mechanical alloys are below the detection limit of XRD. A comprehensive description of the synthesis and characterization of the Al–Mg mechanical alloys has been published elsewhere.[9]

Reequilibrated alloys were produced by completely melting the prepared mechanical alloys in argon and subsequent slow cooling to room temperature. To obtain powders with morphology characteristic to fresh mechanical alloys (particle size distribution, relative surface area), a quantity of annealed material was ball-milled under Ar for 10 minutes. These reequilibrated alloys were found to show no detectable contamination by XRD besides the low levels of ZrO_2 also present in the fresh mechanical alloys.

Thermal Analysis

DSC, DTA, and TGA were performed in a Netzsch Simultaneous Thermal Analyzer STA409 PC. Both DSC and DTA were calibrated for temperature with the melting points of a set of metal standards. The temperature is accurate within ±1 K. The sensitivity of the DSC was calibrated using the known heat capacity of a sapphire standard. Gas flow rates were 10 ml/min for Ar and 50 ml/min for O_2.

Low-temperature subsolidus phase transitions were investigated by DSC in argon and oxygen atmospheres. DSC measurements were carried out using aluminum sample pans, and the maximum temperature was limited to 420°C. Sample sizes were 15–20 mg. Heating rates were varied from 5 to 25 K/min for experiments in Ar. A heating rate of 20 K/min was chosen for the experiments in oxygen.

DTA was used for high-temperature oxidation experiments to prevent damage to the DSC measuring head in case of sample combustion. For DTA, samples of 15–20 mg were contained in Al_2O_3 crucibles and heated at 20 K/min to a final temperature of 1300°C. Initial experiments with the as-prepared mechanical alloys showed that the fine-size fraction gave rise to a strong and somewhat irreproducible baseline; therefore, the samples were screened with a 63-μm sieve before the oxidation experiments, and only the large-size fraction was used.

To analyze intermediate oxidation products, the furnace power was turned off at 700°C and the atmosphere was replaced with argon. The effective cooling rate is estimated to be ≈ 40 K/min. Recovery and analysis of the oxidation products after run completion at 1300°C was not achieved due to strong sintering of the product oxides to the Al_2O_3 crucible used.

Results

Typical DSC traces of the subsolidus transitions are shown in Fig. 1. Mechanical alloys of the same composition ($Al_{0.7}Mg_{0.3}$) were heated to 400°C at 15 K/min in both A_r and O_2. The two measurements are identical within the reproducibility of the instrument. The exothermic effects at 165°C (≈ −15 J/g), 265°C (≈ −12 J/g), and 315°C (≈ −5 J/g) are associated with the formation of the equilibrium intermetallic phases $Al_{12}Mg_{17}$, and Al_3Mg_2 (Refs. 9–12). These effects are superimposed on a very broad exothermically biased background. The total enthalpy difference between a fresh mechanical alloy and a corresponding thermodynamically stable alloy (annealed below the onset of eutectic melting at 450°C) is difficult to determine from these measurements, but has been estimated to be on the order of −100 J/g (Ref. 9).

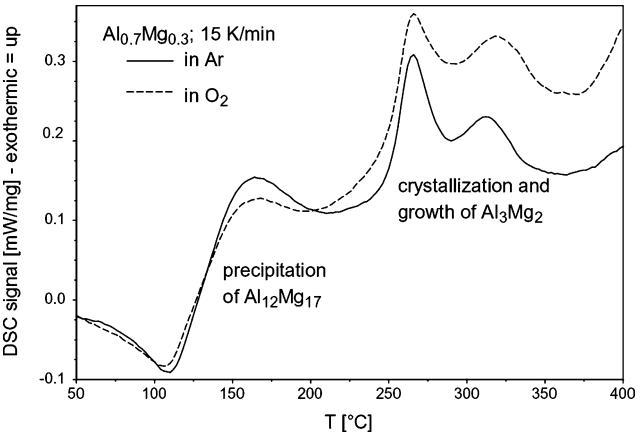

Fig. 1 Low-temperature DSC traces of metastable subsolidus reactions for the mechanical alloy $Al_{0.7}Mg_{0.3}$: ——, argon and – – –, Oxygen.

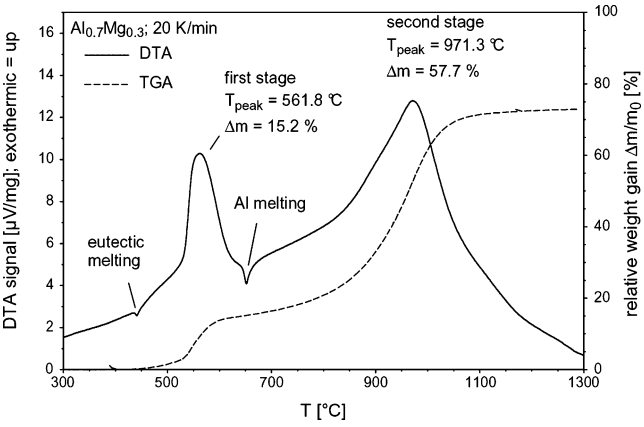

Fig. 2 DTA and TGA traces of $Al_{0.7}Mg_{0.3}$ mechanical alloy heated to 1300°C at 20 K/min in oxygen.

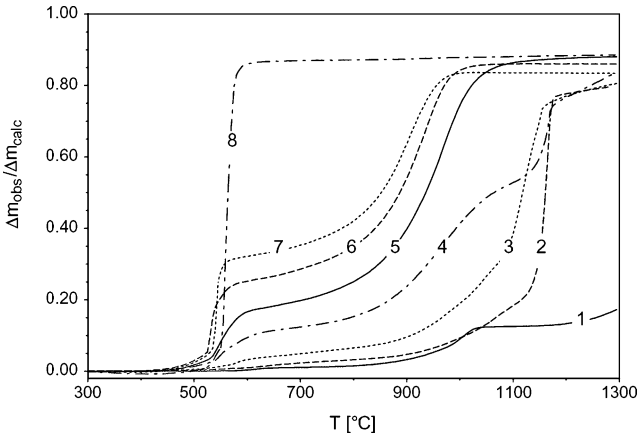

Fig. 3 TGA traces of all investigated mechanical alloys and the pure metal components heated to 1300°C at 20 K/min: 1) Al, 2) $Al_{0.95}Mg_{0.05}$, 3) $Al_{0.9}Mg_{0.1}$, 4) $Al_{0.8}Mg_{0.2}$, 5) $Al_{0.7}Mg_{0.3}$, 6) $Al_{0.6}Mg_{0.4}$, 7) $Al_{0.5}Mg_{0.5}$, and 8) Mg.

Experiments to higher temperatures in oxygen were only conducted using DTA. The observed DTA traces for all alloys are similar to the example shown in Fig. 2. The TGA traces are summarized in Fig. 3. The curves in Fig. 3 have been normalized by the weight gain calculated for complete oxidation of the alloys. Generally, weight changes proceeded in two distinct steps, associated with exothermic heat effects. Details are discussed below. A summary of the temperatures at which the DTA and TGA features were observed

Table 1 Summary of results from the DTA–TGA experiments

	TGA				DTA				
X_{Mg}, at.%	First step[a]	Second step[a] Δm, %	Total[b]	$\Delta m_{obs}/\Delta m^{c}_{calc}$	First peak	Second peak, (endotherms) °C	First step, T_{on}, °C	First step, T_{pk}, °C	Second step, T_{pk}, °C
0	0.93	9.70	15.4	0.17		662.5	573.0	618.2	1011, 1300
5	1.40	63.3	70.2	0.80		654.5	570.0	628.5	1085, 1150
10	3.58	63.3	70.0	0.81		655.8	568.9	585.4	1048, 1124
20	9.50	60.3	71.0	0.84		651.7	537.4	557.0	969, 1170
30	15.2	57.7	72.0	0.87	436.0	651.7	532.9	561.8	971
40	21.1	47.8	69.0	0.86	436.8	650.2	528.9	535.0	939
50	26.1	39.1	65.0	0.83	439.2	649.4	537.7	545.3	910
100	57.8		58.3	0.89			553.8	570.0	

[a]Weight change for the first step was measured below, 660°C and for the second step above 660°C.
[b]Total weight change estimated by weighing sample before and after experiment; includes any weight change that occurred after the end of data acquisition while the DTA furnace was still at high temperature.
[c]Oxidation completeness, Δm_{calc} is weight change calculated for the complete oxidation of the alloy.

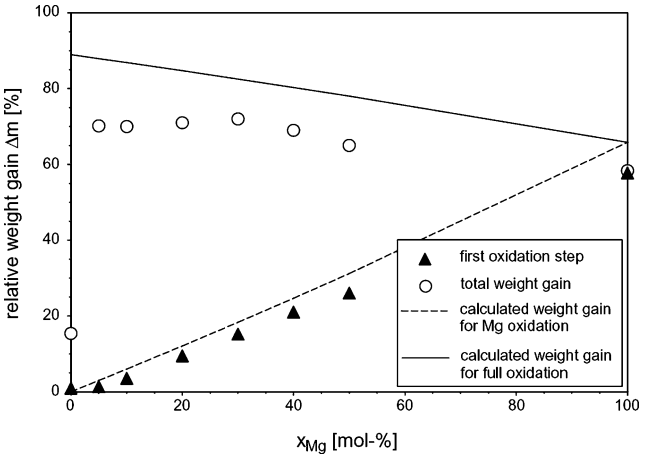

Fig. 4 Comparison: ○, observed total weight change; ▲, partial weight change below 660°C with – – –, calculated weight gains for full oxidation of the Mg component; and ——, entire material.

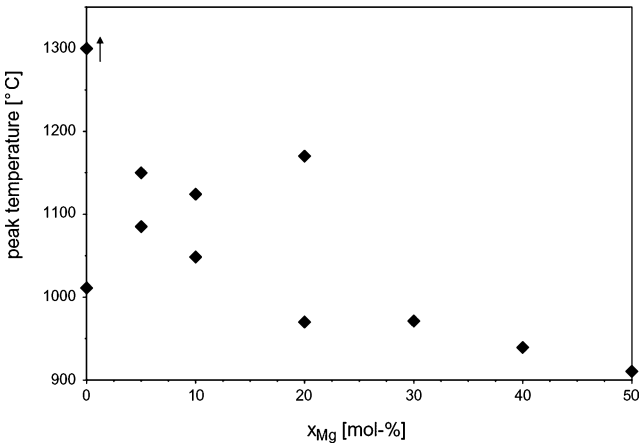

Fig. 5 Peak temperatures for the second oxidation step, where arrow indicates continuing oxidation of pure Al at temperatures higher than the experimental limit of 1300°C.

for different samples is presented in Table 1. Specifically, shown for each alloy are the relative weight increase in the first step using the melting temperature of Al (660°C) as reference temperature, the relative weight increase in the second step, and the total weight gain, measured as the difference of sample weight before and after the experiment. The observed weight gain has been related to the weight gain predicted for complete oxidation of the alloys using the ratio $\Delta m_{obs}/\Delta m_{calc}$. Furthermore, peak temperatures for the endothermic and exothermic effects are shown, as well as onset temperatures for the first oxidation step.

According to the TGA traces, gradual, but noticeable weight gain starts at 400°C. The first oxidation step occurs with an onset temperature decreasing from about 570°C for Al-rich alloys to about 530°C for Mg-rich alloys. Weight continues to increase gradually until the alloys are nearly completely oxidized in a second step, which occurs with poor reproducibility in the range 900–1200°C. The TGA traces showed that the two observed steps are not entirely separated; therefore, the melting temperature of pure Al was used as a reference point to estimate intermediate weight changes. In Fig. 4, the observed weight changes are compared to weight changes calculated under the simplifying assumption that the oxidation of the Mg and Al components can be treated as separate processes. According to Fig. 4, the net weight gain before 660°C loosely correlates with that expected from the complete oxidation of the Mg contained in the alloy. The weight change on full oxidation is always less than calculated, including for oxidation of pure Mg. Generally, the completeness of oxidation of the alloys with Mg concentration less than 30% appears to be decreasing with decreasing Mg concentration. Note that oxidation of pure Al under the same conditions is much less complete. As can be seen in Fig. 3, alloys with Mg concentrations higher than 20% showed no further weight gain above about 1200°C, whereas alloys with 20% Mg and less continued to oxidize at 1300°C.

DTA traces for the samples with Mg concentration greater than 20% show an endothermic effect at the onset of eutectic melting at about 440°C (Table 1). This endothermic peak is not observed for alloys with a lower Mg concentration, or for pure Mg. All of the alloys show a second endothermic peak after the first oxidation stage. A similar peak is also observed for pure Al powder. The peak temperature decreases from 662°C for pure Al to 649°C for the alloy with 50% Mg. The first oxidation step at 530–570°C is accompanied by a strong exothermic effect for all of the alloys and for pure Mg powder. Interestingly, a weak exothermic effect is also observed in the same temperature range for pure Al powder. The second stage of oxidation shows exothermic effects with peak temperatures in the range of 900 –1200°C. Reproducibility of the peak temperature is poor; in addition, Al-rich alloys show multiple peaks. Generally, the temperature of the second oxidation decreases slightly with increasing Mg concentration, as shown in Fig. 5.

XRD analysis of a sample recovered after heating $Al_{0.7}Mg_{0.3}$ to 700°C (above the highest liquidus temperature in the Al–Mg binary system) shows that periclase (MgO) is the only oxide phase at the first stage (Fig. 6). Unmarked peaks in Fig. 6 are due to trace amounts of Al_4C_3, resulting from the presence of stearic acid as processing control agent during mechanical alloying. The scanning electron micrograph in Fig. 7 shows the appearance of the oxide phase in the recovered material. The finely disperse oxide resembles a typical condensation product from a gas-phase reaction. Reproducibility of the first oxidation step for all of the alloys and the good correlation of the observed weight gain with the gain expected based on the Mg contained in the alloys allow one to conclude that MgO is the only oxidation product of the first stage for all of the alloys. The lattice

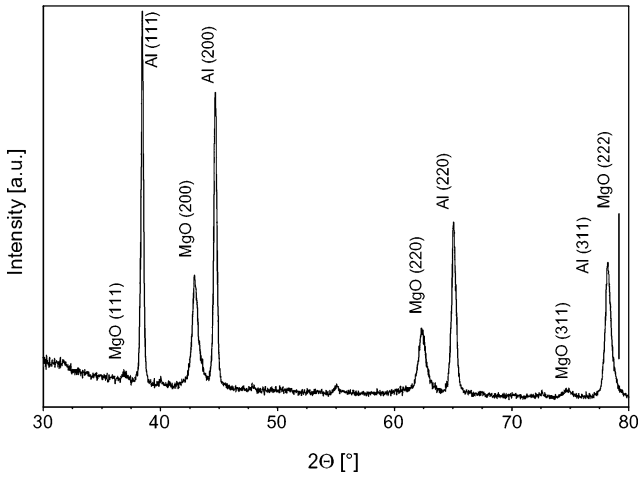

Fig. 6 XRD pattern of the intermediate oxidation product of an $Al_{0.7}Mg_{0.3}$ mechanical alloy.

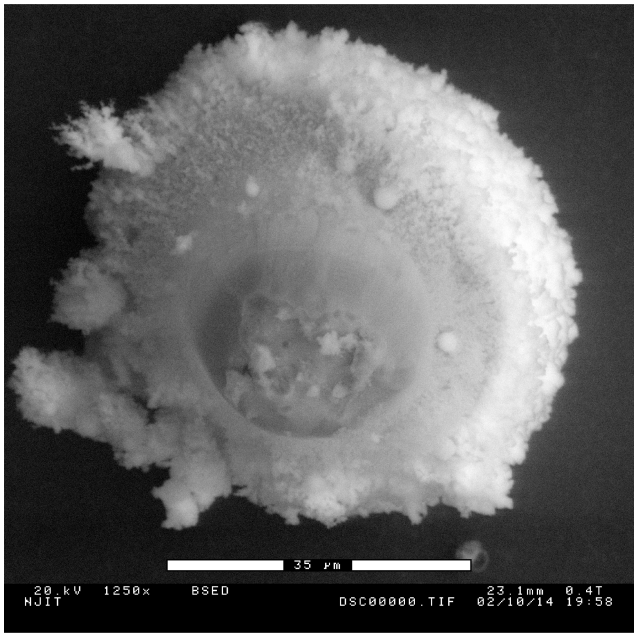

Fig. 7 SEM micrograph of partially oxidized mechanical alloy $Al_{0.7}Mg_{0.3}$ (backscattered electron image): large, rounded metal particle covered with MgO condensation product, darker area in center marks where the particle was attached to its neighbors. The scale bar is 35 μm.

parameter of the aluminum phase in the intermediate oxidation product has been determined to $a_0 = 4.0505 \pm 0.0014$ Å. This corresponds to a residual Mg concentration of approximately 0.2 ± 0.3 at.%. Although the Mg component in the original mechanical alloy is not exclusively contained in the face-centered cubic aluminum phase (see Ref. 9), the drop to near zero from an original 16.3 ± 0.3 at.% in the absence of any Mg containing phases other than MgO signifies near complete removal of the Mg component from the metallic phase at 700°C. The stated compositions were estimated according to previously published linear relations of lattice parameter vs composition in Al–Mg alloys covering Mg concentrations up to 36.8 at.% (Refs. 13 and 14).

For reequilibrated (annealed) alloys that were ground before thermal analysis (see "Experimental"), the DTA–TGA traces observed were qualitatively identical to the experiments on fresh mechanical alloys, signifying substantially identical behavior. However, if the annealed alloys were not ground before heating in O_2, the first oxidation stage occurred very slowly. In these cases, weight increased only gradually, and no peak corresponding to the first oxidation step was observed on the DTA trace.

Discussion

In all alloys, the onset/peak temperature of the first significant oxidation step is about 530–570°C and is nearly independent of Mg concentration. Subsolidus phase changes occurring in mechanical alloys at lower temperatures appear to be unaffected by oxidation. Therefore, the characteristics of these phase changes determined in the DSC experiments in an inert environment (heat effects, reaction rates) could be used in constructing ignition models of mechanically alloyed Al–Mg powders.

Selective oxidation of Mg in Al-based and other Mg-containing alloys has been reported previously.[15] Similar selective oxidation of Mg is observed in the present experiments with all of the samples tested. When judged from the near constant temperature of the first oxidation step (Table 1), from the good correlation of the weight change during this step with the Mg concentration of the alloys (Fig. 4), and from the morphology of the intermediate oxidation products visible by SEM (Fig. 7), the oxidation reaction appears to be controlled mainly by the volatilization of Mg. The equilibrium vapor pressure of magnesium over the pure metal changes from $10^{-3.99}$ bar at 500°C to $10^{-2.06}$ bar at 700°C, whereas the formation of MgO in the presence of oxygen reduces the Mg vapor pressure to $10^{-38.4}$ bar at 500°C and to $10^{-28.5}$ bar at 700°C (values calculated from Refs. 16 and 17). Continuous removal of Mg from the metallic phase by oxidation is, therefore, strongly favored thermodynamically. Even so, the oxidation of Mg is not complete at the temperature where the remainder of the metallic phase melts (second endothermic effect shown in Table 1). The decreasing temperature of this melting peak as a function of initial Mg concentration in the alloy observed in all experiments, consistent with the depression of the Al melting temperature by small fractions of Mg as seen in the equilibrium phase relations,[18] shows that higher initial Mg concentration in the mechanical alloy results in higher residual Mg concentration in the metallic phase after selective Mg oxidation. The low Mg concentration in the Al phase recovered from 700°C as determined from its XRD pattern shows, however, that the Mg loss is near complete at that temperature.

The rate of volatilization of Mg on the particle surfaces is limited by the diffusion rate of Mg in the condensed phase. Therefore, the smaller the effective particle size, the shorter the length scale over which diffusion must occur, and the more rapidly will Mg be removed quantitatively. This is also illustrated by differences in the oxidation behavior observed between fresh mechanical alloys, annealed alloys, and annealed alloys that were ground before thermal analysis. The fresh mechanical alloys have an average apparent particle size on the order of 20 μm, as measured by light scattering and image analysis.[6,9] However, the surface of individual particles is highly developed, and cross-sectioned particles show varying degrees of porosity.[9] This morphology was changed entirely on complete melting during the annealing process. Average particle size increased, any porosity or developed surface was lost, and the specific surface area decreased. The distance over which diffusion must occur increased; therefore, the rate of Mg volatilization, and, in turn, oxidation, was strongly limited. Once the equilibrated material was ground for a short time to reestablish particle morphology and size distribution characteristic of mechanical alloys, oxidation proceeded qualitatively as observed for fresh mechanical alloys, emphasizing the influence of particle size and relative surface area on oxidation rate and completeness.

The observed minor weight change and weak exothermic effect around 570°C in pure Al is consistent with previously published observations.[19] Whether this is an indication of impurities in the metal used, or a genuine property of Al, cannot be decided based on the present observations.

As shown in Table 1 (values of $\Delta m_{obs}/\Delta m_{calc}$) and in Fig. 4 (open circles), none of the investigated alloys showed the full weight gain calculated for complete oxidation. The reasons why even pure Mg did not show the expected completeness are not entirely clear. Oxide or hydroxide impurities in the metal powder could lead to bias in our measurements. Partial removal of MgO condensate by the purge gas in the thermal analysis experiments could account for additional bias. Although this question cannot be answered with

certainty, the observed decrease of the oxidation completeness for alloys with less than 30% Mg, and, more strongly, for pure Al as seen in Fig. 4, is readily understood. Aluminum oxide is known to form a protective layer on metallic surfaces, retarding oxidation,[8,19] whereas magnesium oxide forms a porous layer, which has been reported to have no influence on oxidation rates for Al–Mg alloys with Mg concentrations above 15% (Ref. 20). This is consistent with the observation in the present study that the oxidation reaches a final state only for Mg concentrations of 30% and higher. Figure 5 shows the general trend that the peak temperature of the second oxidation step decreases with increasing Mg concentration of the alloy. Further the high-temperature stage of oxidation occurs in multiple steps for Mg concentrations less than 30%. This is consistent with the notion that the porous Mg oxide promotes diffusion pathways for oxygen, whereas Al oxide encapsulates and protects the metal. Only when the oxide shell is disrupted, for example by stresses caused by differential thermal expansion between oxide and metallic phases, will oxidation proceed rapidly.

Conclusions

Gradual oxidation of mechanical alloys starts in the range of 400–450°C, that is, at higher temperatures than the metastable subsolidus transitions. Subsolidus phase changes are observed equally in both inert and oxidizing environments. No correlation between metastable subsolidus phase transitions and oxidation reactions could be established at heating rates of 20 K/min. It is, therefore, possible to apply the heat effects associated with the metastable subsolidus reactions to ignition models directly.

At least two relatively rapid oxidation steps are observed equally in metastable mechanical Al–Mg alloys and in annealed (thermodynamically stable) Al–Mg alloys. The onset temperature of the first oxidation step decreases from about 570°C for Al-rich alloys to about 530°C for Mg-rich alloys. The onset of rapid oxidation of pure Mg is 554°C. During the first oxidation step, Mg is selectively removed from the alloy to form MgO. This selective oxidation of Mg is controlled by the Mg vapor pressure of the metallic phase. The oxidation is surface controlled; the rate of oxidation is sensitive to specific surface area, particle size distribution, and porosity. Further oxidation of the Mg depleted alloy occurs over a wide range of temperatures. Intermittent surface passivation gives rise to multiple isolated steps in the range of 1000–1200°C for Al-rich materials. Second-stage oxidation in alloys with more than 20 at.% Mg occurs in a single step with a peak temperature as low as 971°C for 30% Mg and 910°C for a Mg concentration of 50 at.%.

In addition, it has been observed that one deciding factor influencing oxidation of Al–Mg mechanical alloys is particle morphology. At the relatively slow heating rates investigated, the metastable nature of the mechanical alloys does not result in detectable changes of the oxidation processes compared to thermodynamically stable Al–Mg alloys. At high heating rates typical for combustion processes ($>10^5$ K/s), however, the contribution of the intermetallic metastable subsolidus transitions to particle self-heating is expected to be significant.

Acknowledgments

This work was supported jointly Office of Naval Research, Grant N00014-00-1-0446 and Crane Division, Naval Surface Warfare Center, Award N0164-02-C-4702. Additional support was provided by New Jersey Commission on Science and Technology, Award 01-2042-007-24.

References

[1]Chan, M. L., Reed, R., and Ciaramitaro, D. A., "Advances in Solid Propellant Formulations," *Solid Propellant Chemistry, Combustion, and Motor Interior Balistics*, Progress in Astronautics and Aeronautics, Vol. 185, AIAA, Reston, VA, 2000, Chap. 1.7, pp. 185–206.

[2]Gany, A., and Netzer, D. W., "Fuel Performance Evaluation for the Solid-Fueled Ramjet," *International Journal of Turbo and Jet Engines*, Vol. 2, No. 2, 1985, pp. 157–168.

[3]Palaszewski, B., and Zakany, J. S., "Metallized Gelled Propellants: Oxygen/RP-1/Aluminum Rocket Combustion Experiments," AIAA Paper 95-2435, July 1995.

[4]Dreizin, E. L., "Phase Changes in Metal Combustion," *Progress in Energy and Combustion Science*, Vol. 26, No. 1, 2000, pp. 57–78.

[5]Shoshin, Y. L., Mudryy, R. S., and Dreizin, E. L., "Preparation and Characterization of Energetic Al–Mg Mechanical Alloy Powders," *Combustion and Flame*, Vol. 128, No. 3, 2002, pp. 259–269.

[6]Dreizin, E. L., and Shoshin, Y. L., "Laminar Lifted Flame Velocity Measurements for Aerosols of Metals and Mechanical Alloys," AIAA Paper 2003-1019, 2003 (submitted for publication).

[7]Schoenitz, M., Dreizin, E. L., and Shtessel E., "Constant Volume Explosions of Aerosols of Metallic Mechanical Alloys and Powder Blends," *Journal of Propulsion and Power*, Vol. 19, No. 3, 2003, pp. 405–412.

[8]Roberts, T. A., Burton, R. L., and Krier, H., "Ignition and Combustion of Aluminum/Magnesium Alloy Particles in O_2 at High Pressures," *Combustion and Flame*, Vol. 92, No. 1–2, 1993, pp. 125–143.

[9]Schoenitz, M., and Dreizin, E. L. "Structure and Properties of Al–Mg Mechanical Alloys," *Journal of Materials Research*, Vol. 18, No. 8, 2003, pp. 1827–1836.

[10]Starink, M. J., and Zahra, A.-M., "β' and β Precipitation in an Al–Mg Alloy Studied by DSC and TEM," *Acta Materialia*, Vol. 46, No. 10, 1998, pp. 3381–3397.

[11]Calka, A., Kaczmarek, W., and Williams, J. S., "Extended Solid Solubility in Ball-Milled Al-Mg Alloys," *Journal of Materials Science and Engineering*, Vol. 28, 1993, pp. 15–18.

[12]Zhang, D. L., Massalski, T. B., and Paruchuri, M. R., "Formation of Metastable and Equilibrium Phases During Mechanical Alloying of Al and Mg Powders," *Metallurgical and Materials Transactions A: Physical Metallurgy and Materials Science*, Vol. 25A, No. 1, 1994, pp. 73–79.

[13]Ellwood, C. E., "Factors Affecting Equilibrium in Certain Aluminium Alloys," *Journal of the Institute of Metals*, Vol. 80, 1952, pp. 605–608.

[14]Luo, H. L., Chao, C. C., and Duwez, P., "Metastable Solid Solutions in Aluminum–Magnesium Alloys," *Transactions of the Metallurgical Society of AIME*, Vol. 230, 1964, pp. 1488–1490.

[15]Surla, K., Valdivieso, F., Pijolat, M., Soustelle, M., and Prin, M., "Kinetic Study of the Oxidation by Oxygen of Liquid Al–Mg 5% Alloys," *Solid State Ionics*, Vol. 143, 2001, pp. 355–365.

[16]Robie, R. A., Hemingway, B. S., and Fisher, J. R., "Thermodynamic Properties of Minerals and Related Substances at 298.15 K and 1 bar (105 Pascals) Pressure and at Higher Temperatures," *Geological Survey Bulletin* 1452, 1978.

[17]Chase, M. W., Jr., *NIST–JANAF Themochemical Tables*, 4th ed., *Journal of Physical and Chemical References Data*, Monograph 9, 1998.

[18]Massalski, T. B. (ed.), Binary Alloy Phase Diagrams, 2nd ed., ASM International, Materials Park, OH, 1990.

[19]Mench, M. M., Kuo, K. K., Yeh, C. L., and Lu, Y. C., "Comparison of Thermal Behavior of Regular and Ultra-fine Aluminum Powders (Alex) Made from Plasma Explosion Process," *Combustion Science and Technology*, Vol. 135, Nos. 1–6, 1998, pp. 269–292.

[20]Breiter, A. L., Maltsev, V. M., and Popov, E. I., "Models of Metal Ignition," *Combustion, Explosion, and Shock Waves*, Vol. 13, 1977, pp. 475–485.